1521-009X/46/11/1767–1775$35.00
DRUG METABOLISM AND DISPOSITION

https://doi.org/10.1124/dmd.118.081877
Drug Metab Dispos 46:1767–1775, November 2018

Special Section – New Models in Drug Metabolism and Transport

Evaluation of Organic Anion Transporter 1A2-knock-in Mice as a Model of Human Blood-brain Barrier[S]

Yamato Sano,[1] Tadahaya Mizuno,[1] Tatsuki Mochizuki, Yasuo Uchida, Mina Umetsu, Tetsuya Terasaki, and Hiroyuki Kusuhara

Graduate School of Pharmaceutical Sciences, the University of Tokyo, Tokyo, Japan (Y.S., T.Mi., T.Mo., H.K.) and Graduate School of Pharmaceutical Sciences, Tohoku University, Miyagi, Japan (Y.U., M.U., T.T.)

Received April 7, 2018; accepted August 17, 2018

ABSTRACT

The present study aimed to establish a humanized mouse model with which to explore OATP1A2-mediated transcellular transport of drug substrates across the blood-brain barrier (BBB) and to evaluate the usefulness of the humanized mice in preclinical studies. Sulpiride, amisulpride, sultopride, and triptans were used as probes to discriminate OATP1A2 and Oatp1a4. We generated a mouse line humanized for OATP1A2 by introducing the coding region downstream of the Oatp1a4 promoter using the CRISPR/Cas9 technique. In the mice generated, OATP1A2 mRNA in the brain was increased corresponding to disappearance of Oatp1a4. OATP1A2 was localized on both the luminal and abluminal sides of the BBB. Unfortunately, study in vivo employing sulpiride, sumatriptan, and zolmitriptan as probes did not indicate any difference in their brain-to-plasma ratio between the control and humanized mice. Quantitative targeted absolute proteomic analysis of the BBB fraction from the humanized mice revealed that almost all analyzed transporters and membrane proteins were expressed at similar levels to those in control mice. The quantitative levels of OATP1A2 differed depending on the peptide quantified, which suggests that incomplete translation or posttranslational modification may occur. The blood-to-brain transport of zolmitriptan, determined by brain perfusion in situ, was 1.6-fold higher in the humanized mice than in the controls, whereas that of sulpiride was not significantly changed. To our knowledge, we established a mouse line humanized for a BBB uptake transporter for the first time. Unfortunately, because of limited impact, there is still room for improvement of the model system.

Introduction

The blood-brain barrier (BBB) plays an important role in excluding various xenobiotics before they reach the central nervous system (CNS). The BBB is one of the most restrictive barriers, with highly developed tight junctions between adjacent endothelial cells and a paucity of fenestra and pinocytotic vesicles, which limits paracellular transport across the endothelial cells. In addition, efflux transporters (such as P-glycoprotein, breast cancer resistance protein, and multi-drug resistance protein 4) pump drugs and other xenobiotic compounds into the blood circulation and also act as a restrictive barrier (Kusuhara and Sugiyama, 2005; Hermann and Bassetti, 2007; Ohtsuki and Terasaki, 2007). Highly specialized uptake systems in the BBB for essential polar nutrients, such as glucose and amino acids, are vital for the brain (Prasad et al., 1999). However, unlike efflux transporters, the involvement of BBB uptake transporters in the penetration of the brain by drugs has not been well characterized in humans. Human organic anion-transporting polypeptide (OATP) 1A2 (the closest murine isoform Oatp1a4 having 72% amino acid sequence homology) is a potentially important uptake transporter allowing drugs to cross the BBB.

Oatp1a4/*Slco1a4* was cloned from rat brain as a homolog of the hepatic multispecific organic anion transporter Oatp1a1 (Noé et al., 1997). Oatp1a4 is abundantly expressed in the brain and liver and localized at both the luminal and abluminal membranes of brain endothelial cells (Gao et al., 1999; Ose et al., 2010). Oatp1a4 shows broad substrate specificity for amphipathic organic anions such as taurocholate, steroid conjugated with glucuronide or sulfate, statins, and [D-penicillamine^{2,5}]-enkephalin (Meier et al., 1997; Eckhardt et al., 1999; Reichel et al., 1999). Brain perfusion studies in situ using Oatp1a4 (−/−) mice suggested that the blood-to-brain transport of pitavastatin, rosuvastatin, taurocholate, and ochratoxin A was

This study was supported by a grant-in-aid for Research on Development of New Drugs from the Japan Agency for Medical Research and Development, AMED [16ak0101030j003] and for Scientific Research (B) [26293032] from the Japan Society for the Promotion of Science.

[1]Y.S. and T.M. contributed equally to this work.

https://doi.org/10.1124/dmd.118.081877.

[S]This article has supplemental material available at dmd.aspetjournals.org.

ABBREVIATIONS: BBB, blood-brain barrier; BSA, bovine serum albumin; CNS, central nervous system; Fw, forward; HEK, human embryonic kidney; LC-MS/MS, liquid chromatography-tandem mass spectrometry; OATP, organic anion transporting peptide; PBS, phosphate-buffered saline; qPCR, reverse-transcription-polymerase chain reaction; QTAP, quantitative targeted absolute proteomics; Rv, reverse; SRM, selected reaction monitoring; TTBS, Tris-buffered saline containing 0.05% Tween 20.

significantly lower in Oatp1a4 (−/−) mice than in wild-type mice, and after microinjection into the cerebral cortex, the brain-to-blood transport of pitavastatin, rosuvastatin, pravastatin, and taurocholate was significantly decreased in Oatp1a4 (−/−) mice compared with that in wild-type mice (Ose et al., 2010). These results suggest that Oatp1a4 can mediate the brain-to-blood and blood-to-brain transport of its drug substrates across the BBB.

OATP1A2 was initially reported to be exclusively expressed at human brain microvessels (Kullak-Ublick et al., 1995). Because OATP1A2 was detected at only the apical membranes of the microvascular endothelium of the BBB, it has been proposed that OATP1A2 mediates uptake of its substrates from the blood side to the brain side (Gao et al., 2000; Lee et al., 2005). OATP1A2 has a wider substrate spectrum than Oatp1a4. In addition to Oatp1a4 substrates mentioned earlier, OATP1A2 transports triptans, such as zolmitriptan and sumatriptan, which likely contribute to their ability to traverse the BBB (Cheng et al., 2012). Because of species differences in substrate recognition between OATP1A2 and Oatp1a4 (Liu et al., 2015), it is difficult to investigate the role of OATP1A2 in drug transport across the BBB using mice. Moreover, extrapolation of human transporter protein data in vitro to in vivo is challenging because of the lack of appropriate models of the human BBB in vitro to measure permeability across cell monolayers. To overcome these obstacles, we generated humanized OATP1A2 transgenic mice (Slco1a4$^{-/-}$; 1A2tg) with insertion of the OATP1A2 cDNA before the sequence of the start codon of Oatp1a4.

Understanding differences in the expression of these two transporters at the BBB could improve predictions of CNS permeability of drug candidates. In this study, we have focused on OATP1A2 to search for other compounds that are substrates of OATP1A2, but not substrates of Oatp1a4 other than triptans, conducted using human embryonic kidney (HEK) 293 cells transfected with OATP1A2. Subsequently, we investigated the influence of the individual human OATP1A2 transporters on the disposition of these OATP1A2-specific substrates in vivo using Oatp1a4-humanized mice.

Materials and Methods

Materials. pCMV6-XL5-OATP1A2 vector was purchased from Origene Technologies (Rockville, MD). pcDNA3.1(+) was purchased from Invitrogen (Carlsbad, CA). Antibodies used in this study are as follows: goat polyclonal anti-OATP1A2 (sc-18428; Santa Cruz Biotechnology, Dallas, TX), mouse monoclonal anti-P-glycoprotein (C219; Signet Laboratories, Dedham, MA), mouse monoclonal anti-β-actin (sc-47778; Santa Cruz Biotechnology). Sumatriptan succinate was purchased from LKT Laboratories (St. Paul, MN). Almotriptan hydrochloride and zolmitriptan were purchased from Toronto Research Chemicals (North York, Canada). Sulpiride, sultopride hydrochloride, and amisulpride were purchased from Wako (Osaka, Japan). Naratriptan hydrochloride and rizatriptan was purchased from Sigma-Aldrich (St. Louis, MO). All other chemicals were of analytical grade.

Cell Culture. Human embryonic kidney 293 (HEK293) cells stably expressing mouse Oatp1a4 (mOatp1a4) were established previously (Ose et al., 2010). For transient expression, pCMV6-XL5-OATP1A2 vector was introduced into HEK293T cells by lipofection with PEI Max 40,000 (Polysciences, Warrington, PA), according to the manufacturer's protocol. The cells were used for the uptake study or Western blotting 48 hours after transfection. These cells were maintained at 37°C under an atmosphere of 5% CO_2 and 95% humidity in Dulbecco's modified Eagle's medium (low glucose; Invitrogen) supplemented with 10% fetal bovine serum.

Transport Study Using cDNA-Transfected Cells In Vitro. A transport study was conducted as reported previously (Ose et al., 2010); 72 hours before the uptake study, cells were seeded in 24-well plates whose wells were coated with poly-L-lysine (50 mg/l) and poly-L-ornithine (50 mg/l) at a density of 1.0×10^5 cells/well. The cells were washed twice and uptake was initiated by addition of Krebs-Henseleit buffer containing the test compounds after preincubation at 37°C for 10 minutes in compound-free Krebs-Henseleit buffer. The Krebs-Henseleit buffer consisted of 23.8 mM $NaHCO_3$, 118 mM NaCl, 4.83 mM KCl, 1.2 mM $MgSO_4$, 0.96 mM KH_2PO_4, 1.53 mM $CaCl_2$, 5 mM D-glucose, and 12.5 mM HEPES adjusted to pH 7.4. The uptake was terminated at the indicated times by the addition of ice-cold buffer and the cells were washed three times. To determine the uptake of compounds, the cells were recovered in Milli-Q water using a cell scraper and disrupted using a Bioruptor (high mode, interval 30 seconds, total 5 min) (UCD-250HSA; Cosmo Bio Co., Tokyo, Japan). A twofold volume of acetonitrile was added for deproteinization, and the specimens were centrifuged for 2 min at 20,000 *g*. The supernatant was subjected to LC-MS/MS analysis. The remaining 20-μl aliquots of cell lysate were used to determine the protein concentration by employing the Lowry method (Lowry et al., 1951) with bovine serum albumin (BSA) as the standard.

Quantification of Test Compounds by LC-MS/MS. The concentrations of compounds in cell suspension, plasma, and brain specimens were measured using an AB Sciex QTRAP 5500 mass spectrometer (Applied Biosystems, Foster City, CA) equipped with a Prominence LC system (Shimadzu, Kyoto, Japan), operated in electrospray ionization mode. The plasma specimens were diluted 100× with Milli-Q water, and the brain was homogenized with a fourfold volume of phosphate-buffered saline (PBS) to obtain a 20% brain homogenate. A twofold volume of acetonitrile was added to the cell suspension, plasma, and brain homogenate for deproteinization. After centrifugation at 20,000 *g* for 2 min, the supernatant was analyzed by LC-MS/MS.

Detailed analytical conditions were summarized in Supplemental Table 1. The mass spectrometer was operated in positive multiple-reaction monitoring mode. The multiple-reaction monitoring precursor/product ion transitions are summarized in Supplemental Table 1. All peak integration and data processing were performed with SCIEX Analyst (v. 1.6.1; Applied Biosystems/MDS SCIEX).

Kinetic Analysis for the Transport Study In Vitro. Transporter-mediated uptake was determined by subtracting the uptake by empty vector transfected cells from that by hOATP1A2-expressing cells. Kinetic parameters for the specific uptake by hOATP1A2 were obtained from eq. 1 (Michaelis-Menten equation):

$$v = \frac{V_{max} \cdot S}{K_m + S} \quad (1)$$

where v, K_m, S, and V_{max} represent the uptake velocity, Michaelis constant, substrate concentration, and maximum transport velocity, respectively. The inhibition constants of naringin, zolmitriptan, and sumatriptan for OATP1A2 were calculated as shown in eq. 2:

$$CL_{uptake\,(+Inhibitor)} = \frac{CL_{uptake\,(control)}}{1 + \frac{I}{K_i}} + P_{dif} \quad (2)$$

where $CL_{uptake\ (+Inhibitor)}$ and $CL_{uptake\ (control)}$ represent the uptake in the presence and absence of inhibitor, respectively, and I, K_i, and P_{dif} represent the inhibitor concentration, inhibition constant, and uptake clearance that remained in the presence of inhibitor, respectively. The fitting using eqs. 1 and 2 was conducted by the iterative nonlinear least-squares method using MULTI software (Yamaoka et al., 1981) and a damped Gauss-Newton algorithm. The substrate concentrations were designed to be below the K_m in the inhibition experiments so that the IC_{50} would approximate K_i.

Experimental Animals. OATP1A2 humanized mice were obtained from Laboratory Animal Resource Center (The University of Tsukuba, Ibaraki, Japan). Wild-type (C57BL/6J) mice were purchased from CLEA Japan (Tokyo, Japan). The mice (8–14 weeks old) were housed in an air-conditioned room set to a 12-hour light/dark cycle and allowed access to water and a standard laboratory diet ad libitum. All experiments were conducted in accordance with guidelines provided by our Institutional Animal Care Committee (Graduate School of Pharmaceutical Sciences, The University of Tokyo, Tokyo, Japan).

Generation of Knock-In Mice by CRISPR/Cas9 Technology. The mouse genomic sequence (5′-GAAAGAGGTTGCAACCCATG-3′) in exon 4 of *Oatp1a4* was selected as a guide RNA target to knock-in the human *OATP1A2* into mouse *Oatp1a4* gene locus. We inserted this sequence into *pX330* plasmid, which carried both guide RNA and Cas9 expression units. This px330 plasmid was a gift from Dr. Feng Zhang (plasmid 42230; Addgene, Cambridge, MA). We named this vector *pX330-mOatp1a4*. In the donor DNA, for homology-directed repair, the human *OATP1A2* cDNA and bovine growth hormone polyadenylation signal were set between the 959-bp 5′ homology arm and the 1177-bp 3′ homology arm. These DNA vectors were dissolved in distilled deionized water and filtered using MILLEX-GV 0.22-μm filter units (Merck Millipore, Burlington, MA). The pregnant mare serum gonadotropin (5 U) and the human chorionic gonadotropin (5 U) were intraperitoneally injected into female C57BL/6J mice (Charles River Laboratories, Kanagawa, Japan) at a 48-hour interval. These mice were mated with male C57BL/6J mice. We collected zygotes from oviducts in mated female mice. A mixture of the *pX330-mOatp1a4* (circular, 5 ng/μl) and the donor DNA (circular, 10 ng/μl) was microinjected into 455 zygotes. Subsequently, the surviving 398 injected zygotes were transferred into oviducts in pseudopregnant ICR females and 79 newborns were obtained. To confirm the

knock-in mutation, we collected genomic DNA from tails and amplified genomic regions including knock-in sequences by PCR with two primer sets: i.e., set 1 (Oatp1a4 5′arm Fw: 5′-CACAAGGGTAGACAGTAAATGATTGAC-3′ and Oatp1a4 5′arm Rv: 5′-CATTATAGGTCTATGCAGTTTGGTTCC-3, upstream of 5′ arm to knocked-in insert), and set 2 (Oatp1a4 3′arm Fw: 5′-GGAACAGAGCTTATAGAGACAAAAGTC-3′ and Oatp1a4 3′arm Rv: 5′-CTATGTTATTGGTTCAGTCTCTAGGAGC-3′, knock-in insert to downstream of 3′ arm). We found that 5 of 79 founders carried a designed knock-in mutation. In addition, we checked random integration of *pX330-mOatp1a4* by PCR with Cas9 detecting primer (Cas9 detection F: 5′-AGTTCATCAAGCCCATCCTG-3′, and Cas9 detection R: 5′-GAAGTTTCTGTTGGCGAAGC -3′) and every five knock-in founders did not carry the Cas9 gene in their genome.

Genotyping of Humanized Mice. Genotyping was performed by PCR analysis using the forward primer (Fw) 5′-GGAGACAATCAGAAGAACAACATGGG-3′, the reverse primer (Rv) 5′-GTTATGGACCACATGTTGGGAACCC-3′, and the other reverse primer (Rv1) 5′-CACCCATTCCACGTACAATATTGCC-3′. PCR with Fw and Rv primers produces a fragment of 330 bp in wild-type and heterozygous mice, whereas PCR with Fw and Rv1 primers produces a fragment of 566 bp in heterozygous and humanized mice.

Quantification of mRNA Expression of hOATP1A2 or mOatp1a4 in the Mouse Brain. The mRNA levels of human OATP1A2, mouse Oatp1a4, and mouse Gapdh were quantified using real-time quantitative polymerase chain reaction (qPCR). Total RNA was isolated from the whole brain of mice using Isogen (Wako Pure Chemicals), and reverse transcription was performed using ReverTra Ace qPCR RT Master Mix with gDNA Remover (Toyobo, Osaka, Japan). qPCR was performed using a Thunderbird SYBR qPCR Mix (Toyobo) and a LightCycler system (Roche Diagnostics, Mannheim, Germany). An external standard curve was generated by dilution of the target PCR product, which was purified by agarose gel electrophoresis. Expression of the target genes in each reaction was normalized to expression of mouse Gapdh. Primers used in this study are listed as follows: 5′-GTTAACATGATCTCCTTCATGCC-3′ and 5′-GGGCAGCTTGTTTGACAGTAAT-3′ (human OATP1A2), 5′-GATCCAGGTCAATGCCTTTATC-3′ and 5′-CCACCAATTAAATATCCGAGGC-3′ (mouse Oatp1a4), 5′-AGAACATCATCCCTGCATCC-3′ and 5′-CACATTGGGGGTAGGAACAC-3′ (mouse Gapdh).

Isolation of Mouse Brain Capillary-Enriched Fraction. A slightly modified method was used for capillary isolation (Ball et al., 2002). In brief, the cortex was homogenized in 0.32 M sucrose (1 g of brain/20 ml of sucrose) using a Polytron homogenizer (Kinematica, Littau-Lucerne, Switzerland). The homogenate was centrifuged at 4°C for 10 min at 2200 *g*, and the resulting pellet was suspended in 25% BSA and centrifuged at 4°C for 10 min at 2200 *g*. The supernatant was decanted and the pellet was washed three times with wash buffer (10 mM Tris-HCl and 0.5 mM dithiothreitol, pH 7.6). The protein concentration was assayed using a bicinchoninic acid method (Smith et al., 1985). These specimens were stored at −80°C until they were analyzed by Western blotting.

Western Blot Analysis. Western blot analysis was conducted as previously described (Mizuno et al., 2015). Specimens were loaded into wells of a 7% SDS-PAGE gel with a 3.75% stacking gel. The molecular weight was determined using Precision Plus Protein Prestained Standards (Bio-Rad, Richmond, CA). Proteins were transferred electrophoretically to a polyvinylidene difluoride membrane (Pall, Port Washington, NY) using a blotter (Bio-Rad) at 100 V for 70 min. The membrane was blocked with 1% skim milk in Tris-buffered saline containing 0.05% Tween 20 (TTBS). After blocking, the membrane was incubated with a 1:1000 dilution of goat anti-hOATP1A2 antibody, a 1:200 dilution of mouse anti-P-glycoprotein antibody, or a 1:500 dilution of mouse anti-β-actin at 4°C overnight, and after three times washing with TTBS, the membrane was incubated with 10,000-fold diluted horseradish peroxidase-conjugated anti-goat or anti-mouse IgG antibody (Amersham Biosciences, Piscataway, NJ) for 40 min at room temperature. Immunoreactivity was detected with an ECL Prime Western Blotting Detection Kit (Amersham Biosciences) after washing with TTBS three times.

Localization of OATP1A2 on Membranes at the BBB by Immunohistochemistry. C57BL/6J mice and the humanized mice were perfused with saline at 6 ml/min for 5 min, the brain was removed and embedded in OCT compound, and then frozen in liquid hexane. Frozen brain was cut into 5-μm-thick sections using a longitudinal orientation of the brain in a cryostat at −20°C. After air drying for 30 min, the tissue slices were fixed in 4% paraformaldehyde at 4°C overnight and then rinsed twice with PBS. Antigens were retrieved by incubating the slices in HistoVT One (Nacalai Tesque, Kyoto, Japan) at 70°C for 20 minutes then rinsing twice with PBS. Nonspecific binding sites on the slices were blocked with 3% BSA in PBS for 30 min, and the sections were stained with a 1:10 dilution of goat anti-hOATP1A2 antibody and a 1:40 dilution of anti-P-glycoprotein antibody in Can Get Signal Immunoreaction Enhancer Solution 1 (Toyobo) and incubated at 4°C overnight, followed by a 1:250 dilution of secondary antibodies [Alexa Fluor 488 donkey anti-goat immunoglobulin G, Alexa Fluor 555 donkey anti-mouse immunoglobulin G (Life Technologies, Carlsbad, CA)] and TO-PRO-3 iodide (Molecular Probes, Eugene, OR) in Can Get Signal Immunoreaction Enhancer Solution 2 (Toyobo, Tokyo, Japan) for 1 hour at room temperature in the dark. The slices were mounted onto glass slides with Vectashield H1000 medium (Vector Laboratories, Burlingame, CA) and were visualized by confocal microscopy using a Leica TCS SP5 II laser-scanning confocal microscope (Leica, Solms, Germany).

Quantitative Targeted Absolute Proteomics of the BBB Fraction from Humanized Mice. Brain capillaries were isolated as described previously with minor modification (Sadiq et al., 2015). We used 25 strokes of a Potter-Elvehjem homogenizer to homogenize the frozen cerebrums from five mice. The capillaries collected from a 20-μm nylon mesh in a 50-ml tube were centrifuged at 2330 *g* (and not 1000 *g*), because 1000 *g* centrifugation is not sufficient to obtain a pellet of capillaries when a 50-ml tube is used. The other experimental conditions and procedures for the isolation of brain capillaries were the same as described previously (Sadiq et al., 2015).

The whole cell lysate of the isolated brain capillaries was digested by lysyl endopeptidase (LysC; Wako Pure Chemicals) and TPCK-treated trypsin (Promega, Fitchburg, WI) as described previously (Sadiq et al., 2015).

The absolute levels of expression of target proteins were determined using a quantitative targeted absolute proteomic (QTAP) analysis as described previously, with minor modifications (Uchida et al., 2013; Sadiq et al., 2015). Briefly, the peptides obtained by trypsin digestion were spiked with a certain amount of stable isotope-labeled (internal standard) peptides, then cleaned up using GL-tip GC and SDB (GL Science, Tokyo, Japan), and then injected into a microLC-MS/MS system. A dilution series of nonlabeled (standard) peptides mixed with the certain amount of internal standard peptides was used for the calibration curve.

The microLC-MS/MS analysis was performed by coupling an Ekspert MicroLC 200 System (Eksigent, Dublin, CA) to a QTRAP 5500 (Sciex) equipped with a Turbo V ion source and 50-μm ID electrode (Sciex). The peptide samples were injected onto a HALO Fused-Core C18 (0.5 × 100 mm, 2.7 μm) column (Eksigent). Mobile phases A and B consisted of 0.1% formic acid in water and 0.1% formic acid in acetonitrile, respectively. The peptides were separated and eluted from the column at 40°C using a linear gradient with a 55-min run time at 10 μl/min. The sequence was as follows: (A:B), 99:1 for 2 min after injection, 70:30 at 32 min, 0:100 at 35 min and up to 37 min, 99:1 at 39 min and up to 55 min, 99:1 for 2 min after injection, 50:50 at 32 min, 0:100 at 35 min and up to 37 min, and 99:1 at 39 min and up to 55 min.

The eluted peptides were simultaneously and selectively detected by means of electrospray ionization in a multiplexed selected reaction monitoring (SRM) analysis. The dwell time was 10 ms per SRM transition. Each molecule was monitored with four sets of SRM transitions (Q1/Q3-1, Q1/Q3-2, Q1/Q3-3, Q1/Q3-4) derived from one set of standard and internal standard peptides. Two peptides (OATP1A2^EG:EGLETNADIIK and OATP1A2^IY:IYDSTTFR) were used for human OATP1A2 protein. The other molecules were monitored with the peptides and SRM transitions reported by Kamiie et al. (2008) and Uchida et al. (2011). Signal peaks over 10,000 counts, which were detected at the same retention time as the internal standard peptides, were defined as positive. When positive peaks were observed in three or four sets of SRM transitions, the molecules were considered to be expressed in brain capillaries, and then the protein expression amounts were determined as the average of three or four quantitative values. The limit of quantification was calculated as described previously (Uchida et al., 2011) with minor modification. We used 10,000 counts of peak area as a cutoff to distinguish whether the target peptides were reliably detected for the quantification or not.

Determination of Blood-to-Brain Transport of Test Compounds Across the BBB Using Brain Perfusion In Situ. Brain perfusion in situ was performed as described previously (Dagenais et al., 2000). In brief, mice were anesthetized by an intraperitoneal injection of sodium pentobarbital (50 mg/kg). The right common carotid artery was catheterized with an SP8 tube mounted on a 30-gauge needle. Before insertion of the catheter, the common carotid artery was ligated caudally. During surgery, the body temperature was maintained by placing the mice on a heated plate (Natsume Seisakusho, Osaka, Japan). A syringe containing perfusion fluid was placed in a pump (Harvard Apparatus Syringe Infusion Pump; Harvard Apparatus, South Natick, MA) and connected to the catheter. Before

perfusion, the thorax of the animal was opened and the heart was cut. Perfusion was started immediately at 1 ml/min. The perfusion fluid consisted of Krebs-Henseleit bicarbonate buffer (25 mM $NaHCO_3$, 118 mM NaCl, 4.7 mM KCl, 1.2 mM $MgSO_4$, 1.2 mM NaH_2PO_4, 1.2 mM $CaCl_2$, and 10 mM D-glucose). The perfusion fluid was bubbled with 95% O_2 and 5% CO_2 for pH control (7.4) and was warmed to 37°C using a water bath. We terminated the perfusion at 1 minute by decapitation. The brain was then removed, and the cortex of the right cerebral hemisphere was placed in a preweighed balance dish (Ina Optika, Osaka, Japan) and weighed. These specimens were stored at −20°C until analyzed by LC-MS/MS.

The apparent volume of brain distribution (V_{brain}) was calculated from the amount of test compound in the right cortex using eq. 3:

$$V_{brain} = \frac{X_{tot}}{C_{perf}} \quad (3)$$

where X_{tot} (drug amount per gram of brain) is the amount of test compound in the right cortex and C_{perf} (concentration in the perfusate).

Pharmacokinetic Study In Vivo and Analysis. C57BL/6J mice and humanized mice (8–14 weeks old) weighing approximately 15–25 g were used for the experiments. Under isoflurane anesthesia, the jugular vein was cannulated with a polyethylene-10 catheter for the administration of drugs. The mice then received a constant intravenous infusion of test compounds at 100 (nmol/min)/kg. The drugs were dissolved in saline. Blood samples were collected from the jugular vein at 30, 60, and 90 min after treatment, the brain was excised immediately after blood collection at 90 min, and then the cortices of the right and left cerebral hemispheres were placed in a preweighed balance dish and weighed. Plasma specimens were obtained by centrifugation of the blood samples (20,000 *g*). These specimens were stored at −20°C until analyzed by LC-MS/MS.

The apparent values of brain-to-plasma concentration ratios ($K_{p,app,brain}$) were calculated from the concentration of test compounds in the plasma and the brain using eq. 4:

$$K_{p,app,brain} = \frac{C_{brain}}{C_{p,90min}} \quad (4)$$

where C_{brain} is the concentration of test compound in the brain at 90 min and $C_{p,90min}$ is the concentration of test compound in the plasma at 90 min.

Statistical Analysis. A two-tailed unpaired Student *t* test and one-way analysis of variance followed by a Tukey multiple comparison test were used to identify significant differences among groups, as appropriate. The data were analyzed using Prism software (GraphPad Software, La Jolla, CA).

Results

Search for Probe Drugs for Evaluating OATP1A2 and Oatp1a4 Differences. To identify the probe sets to evaluate the species differences between OATP1A2 and Oatp1a4, first we searched for new substrates of OATP1A2. Our preliminary study employing oocytes injected with OATP1A2 cRNA suggested that sulpiride, ranitidine, and cibenzoline were the candidates for newly discovered OATP1A2 substrates (Supplemental Fig. 1a). To verify their efficiency as substrates, the uptake of sulpiride, amisulpride, and sulpiride was determined in HEK293T cells transfected with an empty vector, and the cells were transiently expressing OATP1A2 in the absence and presence of naringin, a potent inhibitor of OATP1A2. The latter two were selected because of their structural similarity to sulpiride (Supplemental Fig. 1b). The uptake of sulpiride and amisulpride in the cells expressing OATP1A2 at 10 min was higher than that in the cells transfected with empty vector and was inhibited fully by naringin, while sultopride uptake was not affected by OATP1A2 (Fig. 1A). Next, we investigated the time course for the uptake of sulpiride, amisulpride, cimetidine, and ranitidine. The accumulation of all the tested compounds was greater in the cells expressing OATP1A2 than in those transfected with the empty vector (Fig. 1B). Saturable transport was examined and nonlinear least-squares regression analysis revealed that the K_m and V_{max} for sulpiride for OATP1A2 were 6.68 ± 0.14 μM and 112 ± 1.3 (pmol/min)/mg protein, respectively (Fig. 1C).

From the newly identified and the previously reported OATP1A2 substrates, we selected sulpiride, amisulpride, sumatriptan, and zolmitriptan for further analysis because they are drugs that act in the CNS. To investigate whether they are substrates of Oatp1a4, their uptake was determined in mock and Oatp1a4-expressing HEK293 cells in the absence or presence of naringin. The uptake of all the tested drugs was not significantly different between the mock and Oatp1a4-transfected HEK293 cells, while that of pitavastatin, an Oatp1a4 substrate, was clearly increased in Oatp1a4-expressing HEK293 cells and was inhibited by naringin (Fig. 1D).

Generation and Characterization of Oatp1a4-Humanized Mice. To generate OATP1A2 transgenic mice that express OATP1A2 instead of Oatp1a4 (Oatp1a4-humanized mice), OATP1A2 cDNA was inserted in front of the Oatp1a4 first exon. The starting ATG, stop codon, CRISPR target site, and CRISPR digest site are shown in Fig. 2A and Supplemental Fig. 1a. The result of genotyping with PCR analysis demonstrated that the insertion of OATP1A2 cDNA was successful as designed. Mice of all strains were fertile, with normal life spans, body weights, and brain weights (data not shown).

Quantification of OATP1A2 and Oatp1a4 mRNA in the mouse brain was achieved by qPCR of whole brain from control [OATP1A2 (−/−) Oatp1a4 (+/+)], heterozygous [OATP1A2 (+/−); Oatp1a4 (+/−)), and humanized (OATP1A2 (+/+); Oatp1a4 (−/−)] mice. The expression level of OATP1A2 mRNA in Oatp1a4-humanized mice was about twice as high as that in heterozygous mice, and the expression was lower than the limit of quantitation in control mice (Fig. 2C). By contrast, the levels of expression of Oatp1a4 mRNA showed the opposite pattern to those for OATP1A2 (Fig. 2C). Moreover, an OATP1A2-specific band was detected by Western blotting of the BBB-enriched fraction (defined with P-glycoprotein enrichment) of the humanized mice (Fig. 2D). All of these results were consistent with the genetic design, and we concluded that Oatp1a4-humanized mice were established successfully.

The membrane localization of OATP1A2 in the humanized mice brain was examined immunohistochemically. In Oatp1a4-humanized mice, OATP1A2 signals (Fig. 2E, upper, green) were detected on both sides of the nucleus (Fig. 2E, upper, blue) and overlapped partly with the P-glycoprotein signal (used as a marker of the luminal side of the brain capillaries) (Fig. 2E, upper, red) on one side, while no green signals were seen in frozen sections from the control mice (Fig. 2E, lower). These results indicate that OATP1A2 is expressed on both the luminal and abluminal membranes in the humanized mouse brain capillary endothelial cells as is Oatp1a4.

Infusion Study In Vivo in Control and Oatp1a4-Humanized Mice. To test the Oatp1a4-humanized mice properties as a system to evaluate OATP1A2-mediated drug delivery to the brain, we conducted an infusion study in vivo. Sulpiride or zolmitriptan was administered to the control, the heterozygous, and the humanized mice at a constant rate by intravenous infusion. The concentration in the plasma and the brain was measured with LC-MS/MS and the time-concentration profile, the brain concentration, and the apparent brain-to-plasma concentration ratios were determined. Unfortunately, no variables showed any clear difference between any mouse genotype (Fig. 3, A–C).

Quantitative Targeted Absolute Proteomics of BBB Fractions from Control and Oatp1a4-Humanized Mice. To investigate the effect of substitution of Oatp1a4 by OATP1A2 on the expression of transporters, we conducted quantitative targeted absolute proteomics (QTAP), which is an innovative method to quantify target proteins by employing LC-MS/MS (Ohtsuki et al., 2014). BBB fractions were prepared from control and humanized mice, and the fractions were analyzed by QTAP. As shown in Table 1, almost all of the transporters and membrane proteins analyzed had similar levels of expression between the control and the humanized mice, except for P-glycoprotein, which means

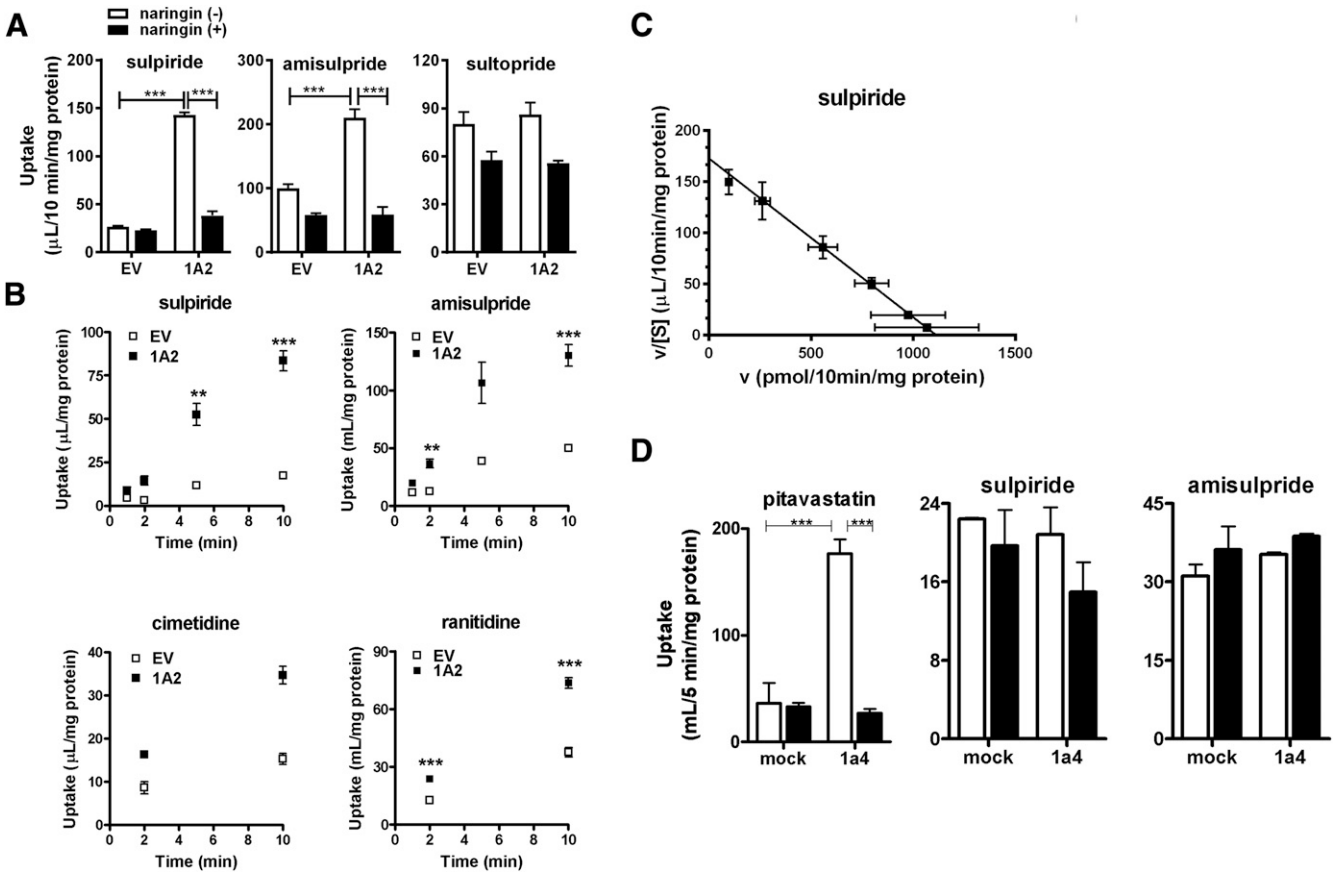

Fig. 1. Search for drug probes to evaluate OATP1A2 and Oatp1a4 differences. (a) The uptake of sulpiride (1 μM), amisulpride (1 μM), and sultopride (1 μM) by HEK293T cells transiently expressing OATP1A2 was examined in the absence (open bar) or presence (closed bar) of naringin (100 μM). (b) Time course of sulpiride (1 μM), amisulpride (1 μM), cimetidine (1 μM), and ranitidine (1 μM) uptake was investigated employing empty vector (open symbols) or HEK293T cells transiently expressing OATP1A2 (closed symbols). (c) Concentration dependence of the uptake of sulpiride (0.1–300 μM). The solid line was fitted by nonlinear regression analysis. (d) The uptake of pitavastatin (1 μM), sulpiride (1 μM), and amisulpride (1 μM) by Oatp1a4-expressing HEK293 cells. Open and filled bars represent naringin (100 μM) (−) and (+), respectively. Each bar or point represents the mean ± S.E., $n = 3$. Statistically significant differences between empty vector and the transporter-expressing cells: $^{**}P < 0.01$; $^{***}P < 0.001$. EV, 1A2, and 1a4 indicate the empty vector, OATP1A2, and Oatp1a4, respectively.

that genetic manipulation did not profoundly affect transporter expression profiles. The expression of P-glycoprotein was 1.5-fold higher in Oatp1a4-humanized mice, and this increase of P-glycoprotein may mask BBB permeability changes in the humanized mice because zolmitriptan is a P-glycoprotein substrate (Bergström et al., 2006). We note that the quantitative concentrations for OATP1A2 differed depending on the peptide quantified: the concentration quantified with OATP1A2^EG, a peptide fragment of OATP1A2 from 273rd E to 283rd K, was 1.52 ± 0.36 fmol/μg protein, while the concentration with OATP1A2^IY, a fragment of OATP1A2 from 591st I to 598th R, was 0.445 ± 0.04 fmol/μg protein. However, the concentrations quantified with these peptides were almost identical in the transient OATP1A2-expression system employed in the uptake study in vitro (Table 2; 10.8 and 10.2 fmol/μg protein for ^EG and ^IY, respectively). Incomplete translation or posttranslational modification of OATP1A2 may occur on the BBB in the humanized mice because OATP1A2^EG is located on the N-terminal side of the transporter, whereas OATP1A2^IY is near the C terminus.

Evaluation of OATP1A2-Mediated Transport in Control and Oatp1a4-Humanized Mice by Brain Perfusion In Situ. We evaluated the brain volume of distribution in the humanized mice with a method for brain perfusion in situ. Sulpiride, sumatriptan, or zolmitriptan was administered to the mice via the right carotid artery at a constant rate, the brain was removed after 1 min of infusion, and the right cerebral hemisphere was analyzed using LC-MS/MS. Diazepam (a flow-rate-limiting drug) was used as a control. The brain uptake of zolmitriptan was increased significantly in Oatp1a4-humanized mice and fully inhibited by naringin. The brain volume of distribution of sumatriptan and sulpiride was not changed significantly between the control and the Oatp1a4-humanized mice, but showed a tendency to increase.

Discussion

Elucidation of the mechanism for BBB transport is an important research theme because it is indispensable for CNS drug targeting. Because the BBB works as a literal "barrier" against drug passage, the function of transporters is essential. However, several lines of evidence indicate that there are species differences. To overcome this problem for modeling, mice humanized for BBB transporters have been generated and characterized recently, such as a mouse line humanized for P-glycoprotein and breast cancer resistance protein (Sadiq et al., 2015; Dallas et al., 2016). However, compared with those humanized for efflux transporters that do exist, to our knowledge, no mice humanized for uptake transporters have existed until now. Therefore, in this study, we generated and characterized a mouse line humanized for OATP1A2 by introducing its coding sequence downstream of the Oatp1a4 (the closest murine isoform) promoter using a CRISPR/Cas9 technique. To our knowledge, this is the first attempt to generate mice humanized for uptake transporters in the BBB, while those for efflux transporters already exist (Sadiq et al., 2015; Dallas et al., 2016). The mice exhibited OATP1A2 expression at the BBB, and the OATP1A2-mediated

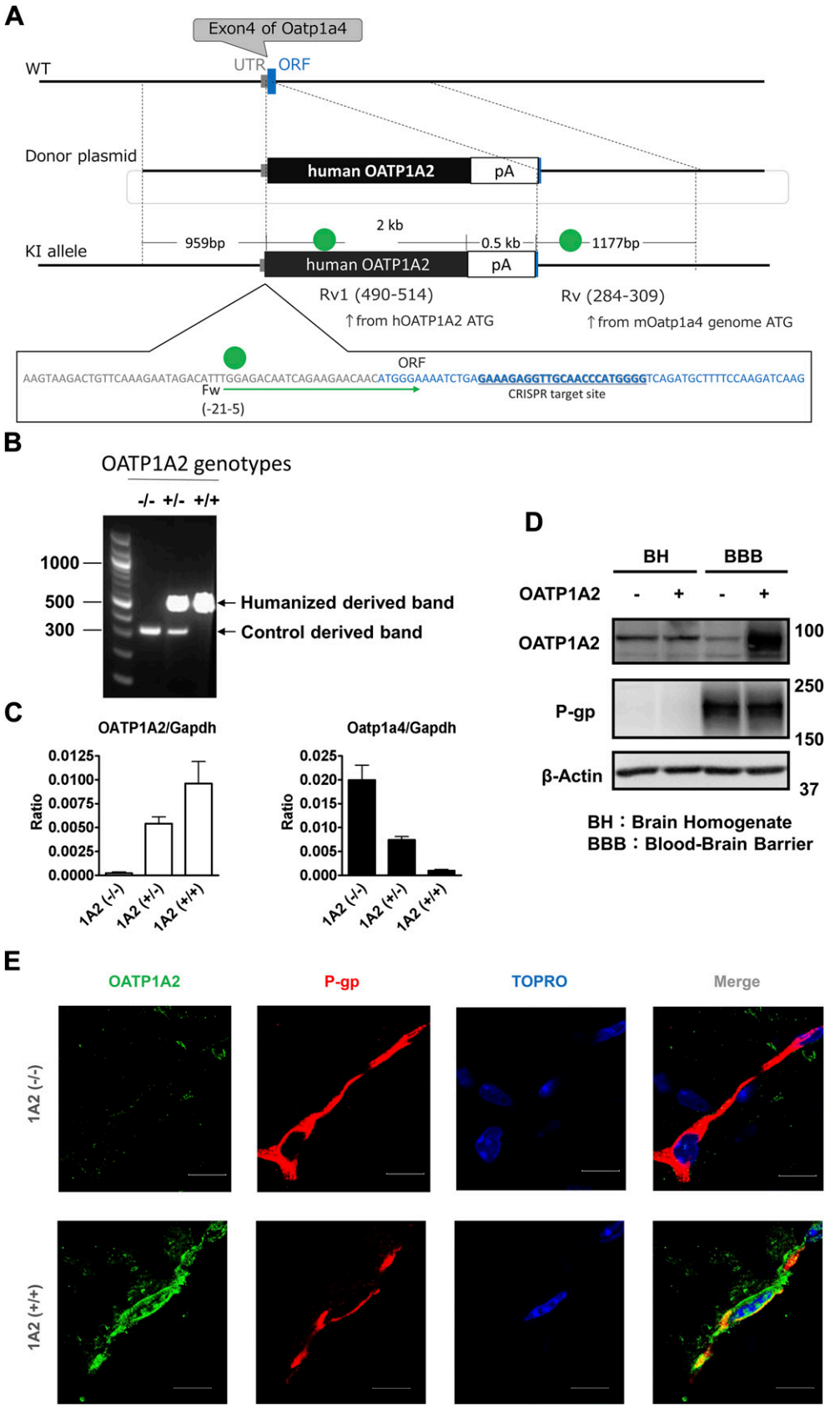

Fig. 2. Establishment and characterization of Oatp1a4-humanized mice. (a) Illustration of the genetic design of Oatp1a4-humanized mice. (b) Identification of control (−/−), heterozygous (+/−), and humanized (+/+) offspring are shown. The design of the primer sets is described in *Materials and Methods*. (c) Quantitative real-time PCR analysis of the brain from the generated mice. OATP1A2 and Oatp1a4 expression were normalized by Gapdh expression. Each bar represents the mean ± S.E. (n = 3). (d) The expression of human OATP1A2, P-gp, and β-actin in brain homogenate (BH) and blood-brain barrier (BBB) of control (−) and humanized mice (+) was detected by Western blotting as described in the *Materials and Methods*. (e) Immunohistochemistry of OATP1A2 with P-gp in brain sections from control (1A2 (−/−), upper) and Oatp1a4-humanized (1A2 (+/+), lower) mice. P-gp was used as a marker of luminal expression: green, OATP1A2; red, P-gp; blue, nuclei stained with TOPRO.

distribution was confirmed by analysis in situ although, not by analysis in vivo, which suggests that OATP1A2 contributes to drug transport into the brain of these mice.

We started with substrate probes to evaluate OATP1A2-specific transport, meaning substrates that can distinguish OATP1A2-mediated transport from that by Oatp1a4 were used. An uptake study employing

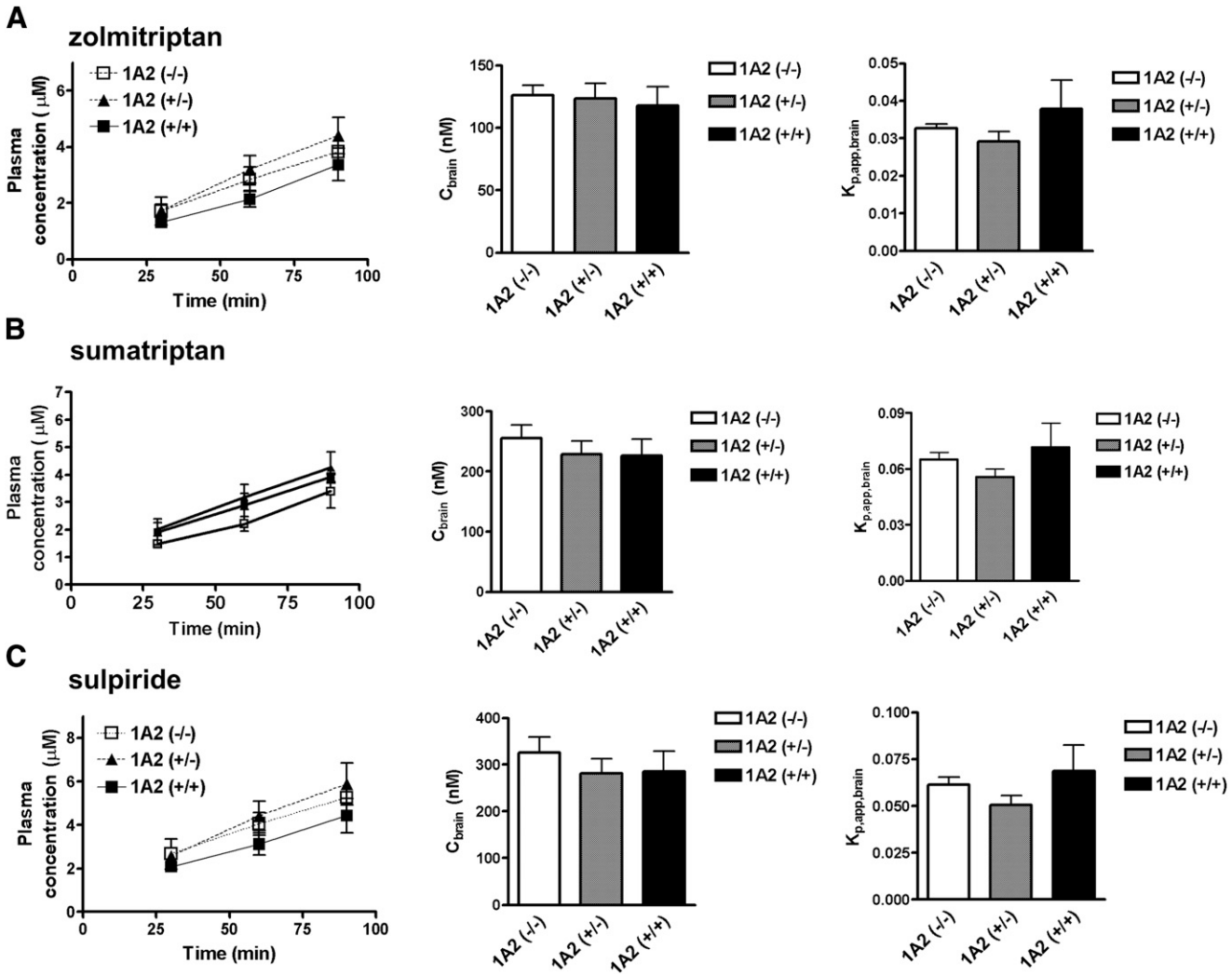

Fig. 3. Study of infusion in Oatp1a4-humanized mice in vivo. Time course of plasma concentrations and brain concentrations within 90 min after the start of drug administration were determined in control (open squares), heterozygous (closed triangles), and humanized (closed squares) mice. Zolmitriptan (a), sumatriptan (c), and sulpiride (c) [100 (nmol/min)/kg] was administered to control (−/−), heterozygous (+/−), and humanized (+/+) mice by intravenous infusion. Blood samples were collected at the designated times. At the end of the experiment, brains were removed. Each point and bar represent the mean ± S.E. (n = 4–6).

OATP1A2-expressing HEK293T cells newly recognized sulpiride and amisulpride as substrates for OATP1A2 (Fig. 1A). By contrast, the newly recognized OATP1A2 substrates mentioned above are not transported by Oatp1a4, which indicates success in nominating another type of probe to evaluate the differences in OATP1A2 and Oatp1a4 transport in addition to the triptans already reported (Liu et al., 2015). We note that sultopride, a benzamide antipsychotic in the same class as sulpiride and amisulpride, was not an OATP1A2 substrate (Supplemental Fig. 1). These results imply that OATP1A2 have defined substrate specificities and that such structural information may facilitate drug design targeting OATP1A2-mediated delivery to the brain.

To achieve humanization, a CRISPR/Cas9 technique was employed and the coding region of human OATP1A2 was introduced into the region downstream of the Oatp1a4 promoter and upstream of the starting codon of the transporter (Fig. 2A). The regulation of OATP1A2 expression was considered to be organized by the mouse Oatp1a4 promoter, and qPCR analysis demonstrated that the expression of Oatp1a4 was inversely correlated with that of OATP1A2 corresponding to the genotypes, which supports the idea that Oatp1a4 promoter regulates OATP1A2 expression in the humanized mice. The results of QTAP analysis employing OATP1A2^EG are consistent with this interpretation, and the quantitative concentration in Oatp1a4-humanized mice was almost the same as that of Oatp1a4 in the control mice (1.52 ± 0.36 vs. 1.52 ± 0.24 fmol/μg protein) (Table 1). By contrast, OATP1A2 concentration quantified with OATP1A2^IY was only a third of that with OATP1A2^EG (0.45 ± 0.04 fmol/μg protein). The difference between the peptides is their location on the protein (Supplemental Fig. 2). OATP1A2^IY is located near the C terminus and represents almost the full length of the transporter, while OATP1A2^EG, on the N-terminal side, possibility reflects not only the full-length protein, but also truncated proteins. We could not reach the conclusion of truncation by analysis of mRNA expression alone, but the proteomic approach with QTAP did support this. The result suggests that incomplete translation or posttranslational modification may occur when human cDNA is inserted simply into the mouse genome.

Impact of OATP1A2 expression on the distribution of OATP1A2 substrates was examined by in vivo and in situ. Unfortunately, employing a study of infusion in vivo revealed no differences in $K_{p,app,brain}$ of the probe drugs between the control and the humanized mice (Fig. 3), although $K_{p,app,brain}$ was greater than volume of the brain capillary lumen (Dagenais et al., 2000), supporting that significant amount of tested drugs distributed to the brain. Therefore, we selected a technique for

TABLE 1

Quantitative targeted absolute proteomics of BBB fraction from Oatp1a4-humanized mice

Transporter protein expression in the brain capillary was quantified as described in *Materials and Methods*. The protein expression level of target molecule was determined as an average and variability (mean ± S.E.) of the quantitative values obtained from different SRM/multiple reaction monitoring (MRM) transitions in three analyses.

Molecular names	Peptide Sequence	Protein Expression Level	
		Control	Humanized
		fmol/μg protein	
OATP1A2^IY	IYDSTTFR	U.L.Q. (<0.076)	0.45 ± 0.04
OATP1A2^EG	EGLETNADIIK	U.L.Q. (<0.39)	1.5 ± 0.36
Oatp1a4	EVATHGVR	1.5 ± 0.24	U.L.Q. (<0.062)
Mdr1a	NTTGALTTR	13 ± 1.2	18 ± 0.5
Oatp1c1	STVTQIER	1.0 ± 0.12	1.1 ± 0.11
Oat3	YGLSDLFR	1.7 ± 0.04	1.7 ± 0.25
Bcrp^SS	SSLLDVLAAR	3.6 ± 0.04	4.3 ± 0.07
Bcrp^EN	ENLQFSAALR	3.0 ± 0.09	3.6 ± 0.12
Mrp4	APVLFFDR	1.0 ± 0.14	1.3 ± 0.17
Glut1	TFDEIASGFR	90 ± 2.3	100 ± 5.2
Taut	EGATPFHSR	U.L.Q. (<1.5)	U.L.Q. (<1.0)
Tfr1	SSVGTGLLLK	3.1 ± 0.16	4.0 ± 0.20
γ-gtp	LFQPSIQLAR	3.2 ± 0.08	4.0 ± 0.29
Na+/K+ ATPase	AAVPDAVGK	48 ± 3.8	56 ± 2.2

Control, BBB fraction from the control mice; Humanized, that from the humanized mice; U.L.Q., under the limit of quantification.

TABLE 2

Quantitative targeted absolute proteomics of OATP1A2-expressing HEK293T cells

Transporter protein expression in OATP1A2-expressing HEK293T cells was quantified as described in *Materials and Methods*. The protein expression level of target molecule was determined as an average and variability (mean ± S.E.) of the quantitative values obtained from different SRM/MRM transitions in three analyses.

Molecular Names	Peptide Sequence	Protein Expression Level	
		EV	OATP1A2
		fmol/μg protein	
OATP1A2^IY	IYDSTTFR	U.L.Q. (<0.073)	11 ± 3.1
OATP1A2^EG	EGLETNADIIK	U.L.Q. (<0.27)	10 ± 2.9
Na+/K+ ATPase	AAVPDAVGK	26 ± 7.5	16 ± 4.5

EV, empty-vector expressing HEK 293T cells; OATP1A2, OATP1A2-expressing HEK293T cells.

brain perfusion in situ to evaluate the short-term BBB permeability. The volume of distribution of zolmitriptan in Oatp1a4-humanized mice was 1.6-fold higher than that in the control mice, and it was sensitive to the OATP1A2 inhibitor, naringin, only in Oatp1a4-humanized mice (Fig. 4). The volume of distribution of zolmitriptan in wild-type mice was close to volume of the brain capillary lumen (Dagenais et al., 2000). These results support the in situ relevance of the species differences in the recognition of substrates by Oatp1a4 and OATP1A2 (Fig. 1A). Unexpectedly, such an effect was quite small or nonexistent for sulpiride and sumatriptan (Fig. 4), although the transport activity of sulpiride by OATP1A2 was rather higher than that of zolmitriptan in an over-expression system (Fig. 1A; Supplemental Fig. 3). The volume of distribution of sumatriptan and sulpiride remains similar to volume of the brain capillary lumen in both wild-type and Oatp1a4-humanized mice.

Taken together, there are two cases among OATP1A2 substrates: *1*) increased BBB permeability with unaltered $K_{p,app,brain}$ (zolmitriptan), *2*) neither BBB permeability nor $K_{p,app,brain}$ was altered (sumatriptan and sulpiride). These discrepancies are unresolved. According to the QTAP analysis (Table 1), the amount of OATP1A2 protein quantified as OATP1A2^IY was one-third of the amount of Oatp1a4 protein. Furthermore, unlike in a previous human brain study (Gao et al., 2000), OATP1A2 was localized on both sides of the BBB in our humanized mice (Fig. 2E). Functional OATP1A2 protein expression was possibly not high enough in the luminal membrane to show a large impact on in situ and in vivo BBB permeability. In addition, expression of OATP1A2 in the abluminal membrane suggests another possibility that OATP1A2 in the luminal membrane also mediates the uptake of its substrate from the CNS side, which facilitates the efflux transport from the CNS side to the blood side as does Oatp1a4 (Ose et al., 2010). Since $K_{p,app,brain}$ is determined not only by the transport in the blood-to-brain direction, but also by that in the opposite direction, such an effect may be able to kinetically blunt the effect of the increased BBB permeability from the blood side on $K_{p,brain}$ (Fig. 2E). To gain an insight into the adaptive regulation of OATP1A2 expression in the BBB, QTAP analysis was conducted. The results show that the transporter expression profile of Oatp1a4-humanized mice was comparable to that of the control mice, which exclude the possibility that induction of transporter proteins overshadowed the impact of OATP1A2 (Table 1). Recent studies demonstrate the importance of posttranslational modification, such as phosphorylation, of the drug transporter protein in its localization and functional activities (Sprowl et al., 2016). Although the posttranslational modification of OATP1A2 in the BBB remains unknown, regulation of

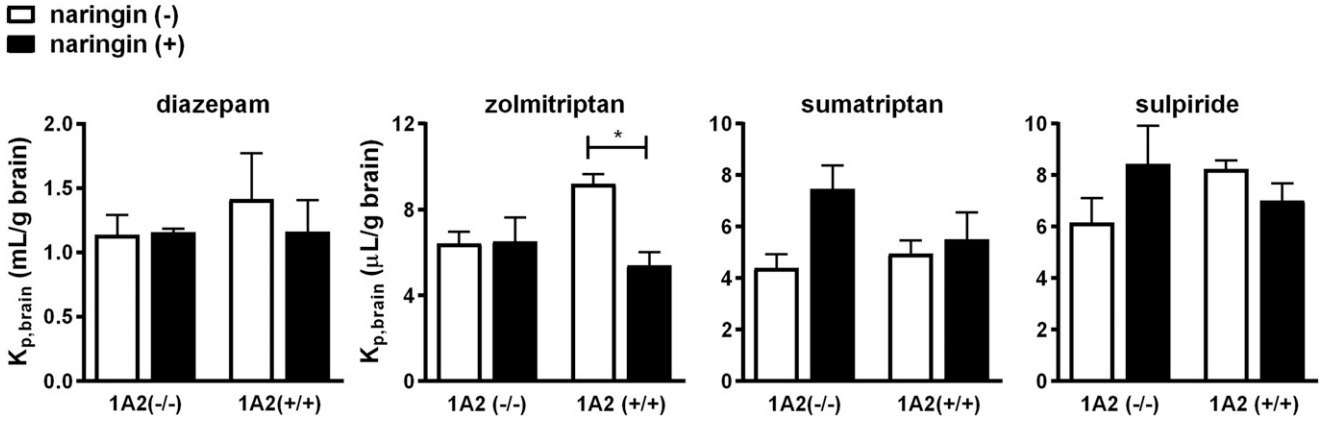

Fig. 4. Study of brain perfusion in situ employing Oatp1a4-humanized mice. The brain volume of distribution was determined using a technique for brain perfusion in situ in control [1A2 (−/−)] or humanized [1A2 (+/+)] mice, with (closed bars) or without (open bars) 100 μM naringin. Diazepam is a flow-rate-limiting drug and used for quality control (QC). The concentrations in the perfusate were 0.5 μM for diazepam and 1 μM for zolmitriptan, sumatriptan, and sulpiride, and perfusion time was 1 min. Each bar represents the mean ± S.E. (n = 4). Significant differences between the groups are denoted by asterisks (*$P < 0.05$).

such posttranslational modifications may be required to acquire sufficiently high activity of OATP1A2 in the BBB in future studies.

In conclusion, we established a mouse line humanized for a BBB uptake transporter for the first time and proposed a method to evaluate OATP1A2-mediated uptake by the BBB. The uptake of zolmitriptan, a serotonin receptor agonist, into the brain by OATP1A2 was demonstrated directly by employing the humanized mice. Further investigation of species differences of transporters and appropriate humanization may help to establish a mouse model with which to evaluate BBB permeability.

Acknowledgments

We appreciate Dr. Kenta Hashizume and Dr. Takami Sarashina (Sekisui medical, Tokyo, Japan) for oocyte experiments. We thank Atsushi Ose (Asahi Kasei Pharma, Tokyo, Japan) for his technical support in the brain perfusion in situ study.

Authorship Contributions

Participated in research design: Sano, M, Kusuhara.
Conducted experiments: Sano, M, Uchida, Umetsu.
Contributed new reagents or analytic tools: Uchida, Umetsu, Terasaki.
Performed data analysis: Sano, M, U, Terasaki, Kusuhara.
Wrote or contributed to the writing of the manuscript: Sano, M, U, Kusuhara.

References

Ball HJ, McParland B, Driussi C, and Hunt NH (2002) Isolating vessels from the mouse brain for gene expression analysis using laser capture microdissection. *Brain Res Brain Res Protoc* **9**:206–213.
Bergström M, Yates R, Wall A, Kågedal M, Syvänen S, and Långström B (2006) Blood-brain barrier penetration of zolmitriptan--modelling of positron emission tomography data. *J Pharmacokinet Pharmacodyn* **33**:75–91.
Cheng Z, Liu H, Yu N, Wang F, An G, Xu Y, Liu Q, Guan CB, and Ayrton A (2012) Hydrophilic anti-migraine triptans are substrates for OATP1A2, a transporter expressed at human blood-brain barrier. *Xenobiotica* **42**:880–890.
Dagenais C, Rousselle C, Pollack GM, and Scherrmann JM (2000) Development of an in situ mouse brain perfusion model and its application to mdr1a P-glycoprotein-deficient mice. *J Cereb Blood Flow Metab* **20**:381–386.
Dallas S, Salphati L, Gomez-Zepeda D, Wanek T, Chen L, Chu X, Kunta J, Mezler M, Menet MC, Chasseigneaux S, et al. (2016) Generation and characterization of a breast cancer resistance protein humanized mouse model. *Mol Pharmacol* **89**:492–504.
Eckhardt U, Schroeder A, Stieger B, Höchli M, Landmann L, Tynes R, Meier PJ, and Hagenbuch B (1999) Polyspecific substrate uptake by the hepatic organic anion transporter Oatp1 in stably transfected CHO cells. *Am J Physiol* **276**:G1037–G1042.
Gao B, Hagenbuch B, Kullak-Ublick GA, Benke D, Aguzzi A, and Meier PJ (2000) Organic anion-transporting polypeptides mediate transport of opioid peptides across blood-brain barrier. *J Pharmacol Exp Ther* **294**:73–79.
Gao B, Stieger B, Noé B, Fritschy JM, and Meier PJ (1999) Localization of the organic anion transporting polypeptide 2 (Oatp2) in capillary endothelium and choroid plexus epithelium of rat brain. *J Histochem Cytochem* **47**:1255–1264.
Hermann DM and Bassetti CL (2007) Implications of ATP-binding cassette transporters for brain pharmacotherapies. *Trends Pharmacol Sci* **28**:128–134.
Kamiie J, Ohtsuki S, Iwase R, Ohmine K, Katsukura Y, Yanai K, Sekine Y, Uchida Y, Ito S, and Terasaki T (2008) Quantitative atlas of membrane transporter proteins: development and application of a highly sensitive simultaneous LC/MS/MS method combined with novel in-silico peptide selection criteria. *Pharm Res* **25**:1469–1483.
Kullak-Ublick GA, Hagenbuch B, Stieger B, Schteingart CD, Hofmann AF, Wolkoff AW, and Meier PJ (1995) Molecular and functional characterization of an organic anion transporting polypeptide cloned from human liver. *Gastroenterology* **109**:1274–1282.
Kusuhara H and Sugiyama Y (2005) Active efflux across the blood-brain barrier: role of the solute carrier family. *NeuroRx* **2**:73–85.
Lee W, Glaeser H, Smith LH, Roberts RL, Moeckel GW, Gervasini G, Leake BF, and Kim RB (2005) Polymorphisms in human organic anion-transporting polypeptide 1A2 (OATP1A2): implications for altered drug disposition and central nervous system drug entry. *J Biol Chem* **280**:9610–9617.
Liu H, Yu N, Lu S, Ito S, Zhang X, Prasad B, He E, Lu X, Li Y, Wang F, et al. (2015) Solute carrier family of the organic anion-transporting polypeptides 1A2- Madin-Darby canine kidney II: a promising in vitro system to understand the role of organic anion-transporting polypeptide 1a2 in blood-brain barrier drug penetration. *Drug Metab Dispos* **43**:1008–1018.
Lowry OH, Rosebrough NJ, Farr AL, and Randall RJ (1951) Protein measurement with the Folin phenol reagent. *J Biol Chem* **193**:265–275.
Meier PJ, Eckhardt U, Schroeder A, Hagenbuch B, and Stieger B (1997) Substrate specificity of sinusoidal bile acid and organic anion uptake systems in rat and human liver. *Hepatology* **26**:1667–1677.
Mizuno T, Hayashi H, and Kusuhara H (2015) Cellular cholesterol accumulation facilitates ubiquitination and lysosomal degradation of cell surface-resident ABCA1. *Arterioscler Thromb Vasc Biol* **35**:1347–1356.
Noé B, Hagenbuch B, Stieger B, and Meier PJ (1997) Isolation of a multispecific organic anion and cardiac glycoside transporter from rat brain. *Proc Natl Acad Sci USA* **94**:10346–10350.
Ohtsuki S, Hirayama M, Ito S, Uchida Y, Tachikawa M, and Terasaki T (2014) Quantitative targeted proteomics for understanding the blood-brain barrier: towards pharmacoproteomics. *Expert Rev Proteomics* **11**:303–313.
Ohtsuki S and Terasaki T (2007) Contribution of carrier-mediated transport systems to the blood-brain barrier as a supporting and protecting interface for the brain; importance for CNS drug discovery and development. *Pharm Res* **24**:1745–1758.
Ose A, Kusuhara H, Endo C, Tohyama K, Miyajima M, Kitamura S, and Sugiyama Y (2010) Functional characterization of mouse Organic anion transporting peptide 1a4 in the uptake and efflux of drugs across the blood-brain barrier. *Drug Metab Dispos* **38**:168–176.
Prasad PD, Wang H, Huang W, Kekuda R, Rajan DP, Leibach FH, and Ganapathy V (1999) Human LAT1, a subunit of system L amino acid transporter: molecular cloning and transport function. *Biochem Biophys Res Commun* **255**:283–288.
Reichel C, Gao B, Van Montfoort J, Cattori V, Rahner C, Hagenbuch B, Stieger B, Kamisako T, and Meier PJ (1999) Localization and function of the organic anion-transporting polypeptide Oatp2 in rat liver. *Gastroenterology* **117**:688–695.
Sadiq MW, Uchida Y, Hoshi Y, Tachikawa M, Terasaki T, and Hammarlund-Udenaes M (2015) Validation of a P-glycoprotein (P-gp) humanized mouse model by integrating selective absolute quantification of human MDR1, mouse Mdr1a and Mdr1b protein expressions with in vivo functional analysis for blood-brain barrier transport. *PLoS One* **10**:e0118638.
Smith PK, Krohn RI, Hermanson GT, Mallia AK, Gartner FH, Provenzano MD, Fujimoto EK, Goeke NM, Olson BJ, and Klenk DC (1985) Measurement of protein using bicinchoninic acid. *Anal Biochem* **150**:76–85.
Sprowl JA, Ong SS, Gibson AA, Hu S, Du G, Lin W, Li L, Bharill S, Ness RA, Stecula A, et al. (2016) A phosphotyrosine switch regulates organic cation transporters. *Nat Commun* **7**:10880.
Uchida Y, Ohtsuki S, Katsukura Y, Ikeda C, Suzuki T, Kamiie J, and Terasaki T (2011) Quantitative targeted absolute proteomics of human blood-brain barrier transporters and receptors. *J Neurochem* **117**:333–345.
Uchida Y, Tachikawa M, Obuchi W, Hoshi Y, Tomioka Y, Ohtsuki S, and Terasaki T (2013) A study protocol for quantitative targeted absolute proteomics (QTAP) by LC-MS/MS: application for inter-strain differences in protein expression levels of transporters, receptors, claudin-5, and marker proteins at the blood-brain barrier in ddY, FVB, and C57BL/6J mice. *Fluids Barriers CNS* **10**:21.
Yamaoka K, Tanigawara Y, Nakagawa T, and Uno T (1981) A pharmacokinetic analysis program (multi) for microcomputer. *J Pharmacobiodyn* **4**:879–885.

Address correspondence to: Hiroyuki Kusuhara, Laboratory of Molecular Pharmacokinetics, Graduate School of Pharmaceutical Sciences, The University of Tokyo, 7-3-1 Hongo, Bunkyo-ku, Tokyo 113-0033, Japan. E-mail: kusuhara@mol.f.u-tokyo.ac.jp